

# Numerical solution of an inverse problem in size-structured population dynamics

Marie Doumic<sup>1</sup>, Benoît Perthame<sup>2,3</sup> and Jorge P Zubelli<sup>4</sup>

<sup>1</sup> Département de Mathématiques et Applications, École Normale Supérieure, INRIA Projet BANG, 45 rue d'Ulm, F 75230 Paris Cedex 05, France

<sup>2</sup> Université Pierre et Marie Curie-Paris 6, UMR 7598 LJLL, BC187, 4, Place Jussieu, F-75252 Paris Cedex 5, and Institut Universitaire de France

<sup>3</sup> INRIA Rocquencourt, Projet BANG, Domaine de Voluceau, BP 105, 78115 Rocquencourt, France

<sup>4</sup> IMPA, Est. D. Castorina 110, Rio de Janeiro, RJ 22460-320, Brazil

E-mail: [doumic@dma.ens.fr](mailto:doumic@dma.ens.fr), [perthame@ann.jussieu.fr](mailto:perthame@ann.jussieu.fr) and [zubelli@impa.br](mailto:zubelli@impa.br)

Received 8 June 2008, in final form 7 December 2008

Published 17 February 2009

Online at [stacks.iop.org/IP/25/045008](http://stacks.iop.org/IP/25/045008)

## Abstract

We consider a size-structured model for cell division and address the question of determining the division (birth) rate from the measured stable size distribution of the population. We propose a new regularization technique based on a filtering approach. We prove convergence of the algorithm and validate the theoretical results by implementing numerical simulations, based on classical techniques. We compare the results for direct and inverse problems, for the filtering method and for the quasi-reversibility method proposed in Perthame and Zubelli (2007 *Inverse Problems* **23** 1037).

(Some figures in this article are in colour only in the electronic version)

## 1. Introduction

The use of size-structured models to describe biological systems has attracted the interest of many authors and has a long standing tradition. In particular, the use of size structures was very well documented and compared to experiments in the 1970s. This led to the survey book [2] and subsequent mathematical analysis (see also references in [3]). Needless to say, in such models it is crucial for the analysis, computer simulation and prediction to calibrate the corresponding model parameters so as to obtain good quantitative results. Indeed, in the inverse problem literature, a number of authors have addressed the calibration of certain structured population models. See, for example, [4–7] and references therein.

In this paper, we consider theoretical and numerical aspects of the inverse problem of determining the division rate coefficient  $B = B(x)$  in the following specific size-structured

model for cell division:

$$\begin{cases} \frac{\partial}{\partial t}n(t, x) + \frac{\partial}{\partial x}n(t, x) + B(x)n(t, x) = 4B(2x)n(t, 2x), & x \geq 0, t \geq 0, \\ n(t, x = 0) = 0, t > 0, \\ n(0, x) = n^0(x) \geq 0. \end{cases} \quad (1)$$

Here, the cell density is represented by  $n(t, x)$  at time  $t$  and size  $x$ . The division rate  $B$  expresses the division of cells of size  $2x$  into two cells of size  $x$ .

By making use of flux cytometry technologies for instance, it is possible to determine cell populations with certain properties as protein content on a large scale of tenths of thousands of cells. In other applications, like coagulation fragmentation equation [8–12], or prion aggregation and fragmentation [13–15], similar equations arise, and much less is known on aggregate size repartition. The division rate  $B(x)$ , in contrast, is not directly measurable.

The long-time behavior of solutions is well known. Indeed, it was proved in [16, 17] that under fairly general conditions on the coefficients, there is a unique solution  $(N, \lambda_0)$  to the following eigenvalue problem:

$$\begin{cases} \frac{\partial}{\partial x}N + (\lambda_0 + B(x))N = 4B(2x)N(2x), & x \geq 0, \\ N(x = 0) = 0, \\ N(x) > 0 \text{ for } x > 0, & \int_0^\infty N(x) dx = 1, \end{cases} \quad (2)$$

where  $\lambda_0 > 0$  and  $N e^{\mu x} \in L^\infty \cap L^1$  for all  $\mu < \lambda_0$ .

It was shown in [16, 18]

$$n(t, x) e^{-\lambda_0 t} \xrightarrow[t \rightarrow \infty]{} m_0 N(x), \quad \text{in } L^1(\mathbb{R}_+, \phi(x) dx),$$

where the weight  $\phi$  is the unique solution to the adjoint problem

$$\begin{cases} -\frac{\partial}{\partial x}\phi + (\lambda_0 + B(x))\phi = 2B(x)\phi\left(\frac{x}{2}\right), & x \geq 0, \\ \phi(x) > 0, & \int_0^\infty \phi(x)N(x) dx = 1. \end{cases} \quad (3)$$

In other words,  $\lambda_0$  is the growth rate of such a system and is usually called ‘Malthus parameter’ in population biology. From [3, 16, 18] we also know that  $\lambda_0$  is related to  $N$  by the relation

$$\lambda_0 = \frac{\int_0^\infty N dx}{\int_0^\infty x N dx}. \quad (4)$$

The question we address here is the following: how can we estimate the division rate  $B$  from knowledge of the steady dynamics  $N$  and  $\lambda_0$ ? The inverse problem thus consists of finding  $B$  a solution to

$$4B(2x)N(2x) - B(x)N(x) = L(x) := \frac{\partial}{\partial x}N(x) + \lambda_0 N(x), \quad x \geq 0, \quad (5)$$

assuming that  $(N, \lambda_0)$  is known, or thanks to (4) that  $N$  is known. As seen in [1], this problem is well-posed if  $N$  satisfies strong regularity properties such as  $\frac{\partial}{\partial x}N(x) \in L^p(\mathbb{R}_+)$  for some  $p \geq 1$ .

However, in practical applications we have only an *approximate* knowledge of  $(N, \lambda_0)$ , given by noisy data  $(N_\varepsilon, \lambda_\varepsilon)$ , with  $N_\varepsilon \in L^2_+(\mathbb{R}_+)$  for instance<sup>5</sup>. This means that we have no

<sup>5</sup> Actually, our knowledge of  $\lambda_0$  is presumably an order of precision higher than that of  $N$ , since the rate  $\lambda_0$  can be estimated independently by means of time information.

way of controlling  $\frac{\partial}{\partial x} N_\varepsilon$ , so we cannot control the precision of a solution  $B_\varepsilon$  to problem (5) when a perturbed  $N_\varepsilon$  replaces  $N$ . Furthermore, it is not even clear whether such a  $B_\varepsilon$  exists.

The question we focus on is then: how to approximate the problem (5) in order to get a solution  $B_\varepsilon$  as close as possible to the exact division rate  $B$ ?

We remark that, in the context of noisy data, the inverse problem under consideration is ill-posed [1] and thus regularization would be required. A natural tool to be invoked from the inverse problem literature would be some kind of Tikhonov regularization method [19, 20]. However, this would lead to computationally intensive problems. Indeed, for each forward problem evaluation a dilation-differential equation of the form (2) would have to be solved.

In [1], two of the present authors proposed a method of regularization consisting of the solution of the following approximate problem:

$$\begin{cases} \alpha \frac{\partial}{\partial y} (B_{\varepsilon,\alpha} N_\varepsilon) + 4B_{\varepsilon,\alpha}(y) N_\varepsilon(y) = B_{\varepsilon,\alpha} \left(\frac{y}{2}\right) N_\varepsilon \left(\frac{y}{2}\right) + \lambda_0 N_\varepsilon \left(\frac{y}{2}\right) \\ \quad + 2 \frac{\partial}{\partial y} \left( N_\varepsilon \left(\frac{y}{2}\right) \right), & y > 0, \\ (B_{\varepsilon,\alpha} N_\varepsilon)(0) = 0, \end{cases}$$

where  $\alpha$  is a regularizing parameter. It was shown that a convergence rate of order  $\sqrt{\varepsilon}$  could be obtained, for  $\alpha = O(\sqrt{\varepsilon})$ , where  $\varepsilon$  is the error on the data  $N$  in an appropriate norm.

The above method of the solution to the inverse problem will be called *quasi reversibility* in accordance with the general spirit of the terminology of [21, 22]. The main goal of this work is to investigate the numerics of such an approach, to consider an alternative technique based on filtering ideas and to compare the performance of the different methods. The alternative technique is also analyzed from the theoretical point of view and estimates are presented.

In this work, we have modified slightly the original regularization equation by writing  $\lambda_{\varepsilon,\alpha}$  instead of  $\lambda_0$  for the reasons we shall explain in the following. Thus, we work with

$$\begin{cases} \alpha \frac{\partial}{\partial y} (B_{\varepsilon,\alpha} N_\varepsilon) + 4B_{\varepsilon,\alpha}(y) N_\varepsilon(y) = B_{\varepsilon,\alpha} \left(\frac{y}{2}\right) N_\varepsilon \left(\frac{y}{2}\right) + \lambda_{\varepsilon,\alpha} N_\varepsilon \left(\frac{y}{2}\right) \\ \quad + 2 \frac{\partial}{\partial y} \left( N_\varepsilon \left(\frac{y}{2}\right) \right), & y > 0, \\ (B_{\varepsilon,\alpha} N_\varepsilon)(0) = 0. \end{cases} \tag{6}$$

Indeed, in order to conserve regularity properties of the solution  $H = BN$  to the inverse problem, we want it to be both in  $L^1(\mathbb{R}_+)$  and in  $L^1(\mathbb{R}_+, x dx)$  in order to express that both the total number of cells and the total biomass are finite. Hence, formal integration of equation (6) gives

$$\lambda_{\varepsilon,\alpha} \int_0^\infty N_\varepsilon dx = \int_0^\infty B_{\varepsilon,\alpha} N_\varepsilon dx, \tag{7}$$

and integration against the weight  $x$  gives

$$-\alpha \int_0^\infty B_{\varepsilon,\alpha} N_\varepsilon dx = 4\lambda_{\varepsilon,\alpha} \int_0^\infty x N_\varepsilon dx - 4 \int_0^\infty N_\varepsilon dx. \tag{8}$$

Hence, we have to choose, according to the eigenvalue theory:

$$\lambda_{\varepsilon,\alpha} = \frac{\int_0^\infty N_\varepsilon dx}{\int_0^\infty x N_\varepsilon dx + \frac{\alpha}{4} \int_0^\infty N_\varepsilon dx}. \tag{9}$$

The choice of  $\lambda_{\varepsilon,\alpha}$  can be understood as a compatibility condition when  $\alpha > 0$  and for  $\alpha = 0$  it tells us that  $(N, \lambda_0)$  is overdetermined data for the inverse problem. Therefore, if we have

*a priori* knowledge on  $\lambda_0$ , we could verify its distance to  $\lambda_{\varepsilon,\alpha}$  as a way of checking the error of the inverse problem solution.

The plan of this work is the following: in section 2, we propose yet another method to regularize the inverse problem, and obtain a convergence rate. The convergence rate turns out to be as good as that in [1]. In section 3, we give a numerical method to solve it and in section 4, we show some numerical simulations so as to compare the accuracy of the different methods.

## 2. Regularization by filtering

### 2.1. Filtering approach

Taking a closer look at equation (5), we see that all the difficulties come from the differential term  $\frac{\partial}{\partial x}N$ . In [1], the choice was to add an equivalent derivative  $\alpha \frac{\partial}{\partial x}(BN)$  to the equation; here in contrast, we choose to regularize it by a convolution method.

For  $\alpha > 0$ , we use the notation

$$\rho_\alpha(x) = \frac{1}{\alpha} \rho\left(\frac{x}{\alpha}\right), \quad \rho \in \mathcal{C}_c^\infty(\mathbb{R}), \quad \int_0^\infty \rho(x) dx = 1, \quad \rho \geq 0, \quad \text{Supp}(\rho) \subset [0, 1], \quad (10)$$

and we replace in (5) the term  $\frac{\partial}{\partial x}N_\varepsilon + \lambda_0 N_\varepsilon$  by

$$\begin{aligned} \left(\frac{\partial}{\partial x}N_\varepsilon + \lambda_{\varepsilon,\alpha}N_\varepsilon\right) * \rho_\alpha(x) &= N_\varepsilon * \left(\frac{\partial}{\partial x}\rho_\alpha + \lambda_{\varepsilon,\alpha}\rho_\alpha\right)(x) \\ &= \int_0^\infty N_\varepsilon(x') \left(\frac{\partial}{\partial x}\rho_\alpha + \lambda_{\varepsilon,\alpha}\rho_\alpha\right)(x - x') dx'. \end{aligned}$$

We now use the notation

$$N_{\varepsilon,\alpha} = N_\varepsilon * \rho_\alpha.$$

In this way, we obtain a smooth term in  $L^2(\mathbb{R}_+)$ . Furthermore,  $N_{\varepsilon,\alpha}$  converges to  $N_\varepsilon$  in  $L^2(\mathbb{R}_+)$  when  $\alpha$  tends to zero. We now have to consider the following problem:

find  $B_{\varepsilon,\alpha}$  solution of

$$4B_{\varepsilon,\alpha}(2x)N_{\varepsilon,\alpha}(2x) - B_{\varepsilon,\alpha}(x)N_{\varepsilon,\alpha}(x) = \frac{\partial}{\partial x}N_{\varepsilon,\alpha} + \lambda_{\varepsilon,\alpha}N_{\varepsilon,\alpha}(x), \quad x \geq 0. \quad (11)$$

As in equation (6), for the quasi-reversibility method, we need to choose  $\lambda_{\varepsilon,\alpha}$  appropriately. Indeed, we perform the same manipulations leading to equation (9) to get

$$\lambda_{\varepsilon,\alpha} = \frac{\int_0^\infty N_{\varepsilon,\alpha}(x) dx}{\int_0^\infty x N_{\varepsilon,\alpha}(x) dx}. \quad (12)$$

By theorem appendix A.3 (see the appendix), we know that the problem in equation (11) has a unique solution  $B_{\varepsilon,\alpha} \in L^2(\mathbb{R}_+, N_{\varepsilon,\alpha} dx)$ .

### 2.2. Estimates for the filtering approach

The main result of this section establishes an estimate for the regularization of the inverse problem by means of the filtering method described above.

**Theorem 2.1.** *Suppose that  $N \in H^2(\mathbb{R}_+)$  and  $B \in L^\infty(\mathbb{R}_+)$ ,  $B \geq 0$  verify (2). Let  $\varepsilon > 0$  and  $N_\varepsilon \in L^2(\mathbb{R}_+)$ ,  $N_\varepsilon(x) > 0$  for  $x > 0$ , such that*

$$\|N_\varepsilon - N\|_{L^2(\mathbb{R}_+)} \leq \varepsilon \|N\|_{L^2(\mathbb{R}_+)}.$$

Let  $B_{\varepsilon,\alpha} \in L^2(\mathbb{R}_+, N_{\varepsilon,\alpha}^2 dx)$  be the unique solution of (10) and (11). We have the following estimate:

$$\|B_{\varepsilon,\alpha} - B\|_{L^2(N_{\varepsilon,\alpha}^2 dx)} \leq C(\alpha + |\lambda_{\varepsilon,\alpha} - \lambda_0|) \|N\|_{H^2(\mathbb{R}_+)} + C\left(1 + \frac{1}{\alpha}\right) \|N_{\varepsilon} - N\|_{L^2(\mathbb{R}_+)}, \quad (13)$$

where  $C$  is a constant depending only on  $\|B\|_{L^\infty}$ ,  $\|B_{\varepsilon,\alpha}\|_{L^\infty}$  and the regularizing function  $\rho$ .

This theorem relies on a first estimate.

**Proposition 2.2.** Using the same notations as in theorem 2.1, we have

$$\begin{aligned} \|B_{\varepsilon,\alpha} N_{\varepsilon,\alpha} - BN\|_{L^2(dx)}^2 &\leq C(1 + \lambda_0^2) \left(1 + \frac{1}{\alpha^2}\right) \|N_{\varepsilon} - N\|_{L^2(dx)}^2 \\ &\quad + C(\alpha^2 + |\lambda_{\varepsilon,\alpha} - \lambda_0|^2) \|N\|_{H^2(\mathbb{R}_+)}^2, \end{aligned} \quad (14)$$

where  $C$  depends only on the regularizing function  $\rho$ .

**Proof of proposition 2.2.** Denote by  $Q = B_{\varepsilon,\alpha} N_{\varepsilon,\alpha} - BN$ ,  $R = N_{\varepsilon,\alpha} - N$  and  $\delta = \lambda_{\varepsilon,\alpha} - \lambda_0$ . From equations (2) and (11),  $Q$  verifies

$$\begin{cases} \frac{\partial}{\partial x} R(x) + \lambda_0 R(x) + \delta N_{\varepsilon,\alpha}(x) + Q(x) = 4Q(2x), & x \geq 0, \\ Q(x=0) = 0. \end{cases} \quad (15)$$

(Since  $N_{\varepsilon,\alpha} \in H^1(\mathbb{R}_+)$ , the definition of  $Q(x=0)$  is not ambiguous.) Multiplying this equation by  $Q(2x)$  and integrating on the interval  $(0, y)$  yields

$$\begin{aligned} 4 \int_0^y Q(2x)^2 dx &= \int_0^y Q(2x) \frac{\partial}{\partial x} R(x) dx + \lambda_0 \int_0^y Q(2x) R(x) dx \\ &\quad + \delta \int_0^y Q(2x) N_{\varepsilon,\alpha}(x) dx + \int_0^y Q(2x) Q(x) dx. \end{aligned}$$

From the Cauchy–Schwarz inequality, after the change of variables  $x \rightarrow 2x$ , we have

$$\begin{aligned} 4 \int_0^y Q(2x)^2 dx &\leq \frac{1}{2} \int_0^y \left(\frac{\partial}{\partial x} R\right)^2(x) dx + \frac{1}{2} \int_0^y Q(2x)^2 dx + \frac{\lambda_0}{2} \int_0^y K R(x)^2 dx \\ &\quad + \frac{\lambda_0}{2} \int_0^y \frac{Q(2x)^2}{K} dx + \frac{|\delta|^2}{2} \int_0^y N_{\varepsilon,\alpha}(x)^2 dx \\ &\quad + \frac{1}{2} \int_0^y Q(2x)^2 dx + \frac{1}{2} \int_0^y Q(2x)^2 dx + \int_0^{\frac{y}{2}} Q(2x)^2 dx, \end{aligned}$$

where  $K$  is an arbitrary constant. We take, for instance,  $K = \lambda_0$  and obtain

$$\begin{aligned} \|B_{\varepsilon,\alpha} N_{\varepsilon,\alpha} - BN\|_{L^2}^2 &\leq \left\| N_{\varepsilon} * \frac{\partial}{\partial x} \rho_{\alpha} - \frac{\partial}{\partial x} N \right\|_{L^2}^2 + \lambda_0^2 \|N_{\varepsilon} * \rho_{\alpha} - N\|_{L^2}^2 \\ &\quad + |\lambda_{\varepsilon,\alpha} - \lambda_0|^2 \|N_{\varepsilon} * \rho_{\alpha}\|_{L^2}^2. \end{aligned} \quad (16)$$

The last two terms of this inequality are easy to estimate, writing

$$\begin{aligned} \|N_{\varepsilon} * \rho_{\alpha} - N\|_{L^2} &\leq \|N_{\varepsilon} * \rho_{\alpha} - N * \rho_{\alpha}\|_{L^2} + \|N * \rho_{\alpha} - N\|_{L^2} \\ &\leq C(\|N_{\varepsilon} - N\|_{L^2} + \alpha \|N\|_{H^1}) \end{aligned} \quad (17)$$

and

$$\|N_{\varepsilon} * \rho_{\alpha}\|_{L^2} \leq C \|N\|_{L^2}.$$

It remains to evaluate the first term on the right-hand side of inequality (16). We write

$$\left\| N_\varepsilon * \frac{\partial}{\partial x} \rho_\alpha - \frac{\partial}{\partial x} N \right\|_{L^2}^2 \leq 2 \left\| N_\varepsilon * \frac{\partial}{\partial x} \rho_\alpha - N * \frac{\partial}{\partial x} \rho_\alpha \right\|_{L^2}^2 + 2 \left\| N * \frac{\partial}{\partial x} \rho_\alpha - \frac{\partial}{\partial x} N \right\|_{L^2}^2.$$

By a convolution estimate we evaluate the first term as

$$\left\| N_\varepsilon * \frac{\partial}{\partial x} \rho_\alpha - N * \frac{\partial}{\partial x} \rho_\alpha \right\|_{L^2(\mathbb{R}_+, dx)}^2 \leq \|N_\varepsilon - N\|_{L^2(\mathbb{R}_+, dx)}^2 \left\| \frac{\partial}{\partial x} \rho_\alpha \right\|_{L^1}^2.$$

Since  $\int_0^\infty \left| \frac{\partial}{\partial x} \rho_\alpha(x) \right| dx = \frac{1}{\alpha} \int_0^\infty \left| \frac{\partial}{\partial x} \rho(y) \right| dy$ , we have

$$\left\| N_\varepsilon * \frac{\partial}{\partial x} \rho_\alpha - \frac{\partial}{\partial x} N \right\|_{L^2(\mathbb{R}_+, dx)}^2 \leq \frac{C(\rho)}{\alpha^2} \|N_\varepsilon - N\|_{L^2(\mathbb{R}_+, dx)}^2 + 2 \left\| N * \frac{\partial}{\partial x} \rho_\alpha - \frac{\partial}{\partial x} N \right\|_{L^2(\mathbb{R}_+, dx)}^2.$$

To evaluate the last term  $\left\| N * \frac{\partial}{\partial x} \rho_\alpha - \frac{\partial}{\partial x} N \right\|_{L^2}^2$ , we extend to  $\mathbb{R}$  the functions  $N$  and  $\frac{\partial}{\partial x} N$  by zero and consider their Fourier transforms. We denote  $\hat{f}(\xi)$  the Fourier transform of  $f \in L^2(\mathbb{R}_+)$  at  $\xi$ , where  $f$  is extended as zero on  $\mathbb{R}_-$ . We obtain by Fourier analysis

$$\left\| N * \frac{\partial}{\partial x} \rho_\alpha - \frac{\partial}{\partial x} N \right\|_{L^2(\mathbb{R}_+, dx)}^2 = \left\| i \xi \hat{N} \hat{\rho}_\alpha - i \xi \hat{N} \right\|_{L^2(\mathbb{R}_+, dx)}^2 \leq \int_{-\infty}^\infty |\hat{N}(\xi)|^2 |\xi|^4 \frac{|\hat{\rho}_\alpha(\xi) - 1|^2}{|\xi|^2} d\xi.$$

Now, from the definition of  $\rho_\alpha$ , we have  $\hat{\rho}_\alpha(\xi) = \hat{\rho}(\alpha\xi)$ . Thus,

$$\left\| \frac{(\hat{\rho}_\alpha(\xi) - 1)^2}{\xi^2} \right\|_{L^\infty(\mathbb{R})} = \alpha^2 \left\| \frac{(\hat{\rho}(\xi') - 1)^2}{\xi'^2} \right\|_{L^\infty(\mathbb{R})}.$$

Since  $\int \rho(x) dx = 1$ , we have  $\hat{\rho}(0) = 1$ , and because  $\hat{\rho} \in \mathcal{S}(\mathbb{R})$  the term  $(\hat{\rho}(\xi) - 1)/\xi$  is bounded. Thus,

$$\left| \frac{\hat{\rho}_\alpha(\xi) - 1}{\xi} \right|^2 \leq C(\rho) \alpha^2, \tag{18}$$

where  $C(\rho)$  only depends on the regularization function  $\rho$ . This implies that

$$\left\| N * \frac{\partial}{\partial x} \rho_\alpha - \frac{\partial}{\partial x} N \right\|_{L^2(\mathbb{R}_+, dx)}^2 \leq C(\rho) \alpha^2 \|N\|_{H^2(\mathbb{R}_+)}^2.$$

Going back to (16) we conclude the proof of proposition 2.2. □

We can now prove theorem 2.1. We write

$$\|B_{\varepsilon, \alpha} - B\|_{L^2(N_\varepsilon^2 dx)} \leq \|B_{\varepsilon, \alpha} N_\varepsilon - B_{\varepsilon, \alpha} N_{\varepsilon, \alpha}\|_{L^2(\mathbb{R}_+)} \tag{19}$$

$$+ \|B_{\varepsilon, \alpha} N_{\varepsilon, \alpha} - BN\|_{L^2(\mathbb{R}_+)} + \|BN - BN_\varepsilon\|_{L^2(\mathbb{R}_+)}. \tag{20}$$

We evaluate each term on the right-hand side of this inequality. From equation (17) we have that there exists a constant  $C$  depending only on  $\rho$  such that

$$\|N_\varepsilon - N_{\varepsilon, \alpha}\|_{L^2} \leq \|N_\varepsilon - N\|_{L^2} + \|N - N_{\varepsilon, \alpha}\|_{L^2} \leq C(\|N_\varepsilon - N\|_{L^2} + \alpha \|N\|_{H^1}),$$

so the first term on the right-hand side of inequality (19) gives

$$\|B_{\varepsilon, \alpha} N_\varepsilon - B_{\varepsilon, \alpha} N_{\varepsilon, \alpha}\|_{L^2(\mathbb{R}_+)} \leq C \|B_{\varepsilon, \alpha}\|_{L^\infty} (\|N_\varepsilon - N\|_{L^2} + \alpha \|N\|_{H^1}).$$

The second term on the right-hand side of inequality (19) is estimated by proposition 2.2. Namely, for a constant (still denoted by  $C$ ) only depending on  $\rho$  and  $\lambda_0$ , one has

$$\|B_{\varepsilon, \alpha} N_{\varepsilon, \alpha} - BN\|_{L^2(\mathbb{R}_+)} \leq C \left(1 + \frac{1}{\alpha}\right) \|N_\varepsilon - N\|_{L^2(dx)} + C(\alpha + |\lambda_{\varepsilon, \alpha} - \lambda_0|) \|N\|_{H^2(\mathbb{R}_+)}.$$

The third term on the right-hand side of inequality (19) is simply evaluated by

$$\|BN - BN_\varepsilon\|_{L^2(\mathbb{R}_+)} \leq \|B\|_{L^\infty} \|N - N_\varepsilon\|_{L^2(\mathbb{R}_+)}.$$

Collecting these three inequalities we get equation (13).

### 3. Numerical solution of the inverse problem

This section is concerned with the numerical aspects of the solution of the inverse problem. In order to do that we start with a description of the solution to the direct one in section 3.1.

#### 3.1. Direct problem

In the direct problem, we assume we know the proliferation rate  $B$ , we look for  $N$  and  $\lambda_0 > 0$  solutions of (2). For this purpose, we solve the time-dependent problem (1) and look for a steady dynamics. As already said, this problem is well-posed (see for instance [3]) and it was proved in [18] that solutions grow at an exponential rate toward  $\rho N(x)e^{\lambda_0 t}$  with  $\rho = \int_0^\infty n(0, x)\phi(x) dx$ , recalling the notation in (3). Furthermore, under more restrictive conditions it was shown in [16] that there exists constants  $\mu > 0$  and  $C(n^0) > 0$ , such that

$$\|n(t, x) e^{-\lambda_0 t} - \rho N(x)\|_{L^1(\mathbb{R}_+, \phi(x) dx)} \leq C e^{-\mu t}.$$

To solve it numerically, we discretize the problem (1) along a regular grid, denote by  $\Delta t$  the time step and by  $\Delta x = L/I$  the spatial step, where  $I$  denotes the number of points and  $L$  the computational domain length:  $x_i = i \Delta x$ ,  $0 \leq i \leq I$ .

We use an upwind finite volume method (cf [23–25])

$$n_i^k = \frac{1}{\Delta x} \int_{x_{i-\frac{1}{2}}}^{x_{i+\frac{1}{2}}} n(k \Delta t, y) dy, \quad \frac{1}{\Delta t} \int_0^{\Delta t} n(k \Delta t + s, x_{i+\frac{1}{2}}) ds \approx n_i^k.$$

For the time discretization, we use a marching technique. We choose the time step  $\Delta t$  so as to satisfy the largest possible CFL stability criteria  $\theta := \frac{\Delta t}{\Delta x} = 1$ .

The numerical scheme is given, for  $i = 1, \dots, I$ , by  $n_0^k = 0$  and

$$\frac{n_i^{k+1} - n_i^k}{\Delta t} + \frac{n_i^k - n_{i-1}^k}{\Delta x} + B_i n_i^{k+1} = B_{2i-1} n_{2i-1}^k + 2B_{2i} n_{2i}^k + B_{2i+1} n_{2i+1}^k, \quad (21)$$

with the convention that  $n_j = 0$  for  $j > I$ . For stability reasons, we have used an implicit method for the division term on the lhs and explicit for the rhs of the equation. The specific form for the rhs is simply motivated by the need of also dividing cells of odd labels. The point being that if we used only the contribution  $4B_{2i} n_{2i}^k$  we would miss the contributions from the odd labeled sizes. The reason for choosing the weights 1, 2, and 1 is an arbitrary one, based on symmetry and analogy with centered differences.

According to the power algorithm, we do not keep  $n^{k+1}$  from (21) but rather renormalize it as

$$\tilde{n}^{k+1} = \frac{n^k}{\Delta x \sum_{j=1}^I n_j^k}.$$

It is standard, for these positive matrices arising in (21), that

$$\lim_{k \rightarrow \infty} \tilde{n}^{k+1} = N, \quad \sum_{i=1}^I N_i = 1, \quad N_i > 0,$$

where  $N$  is the dominant eigenvector for the problem

$$\frac{N_i - N_{i-1}}{\Delta x} + (\lambda_0 + B_i) N_i = B_{2i-1} N_{2i-1} + 2B_{2i} N_{2i} + B_{2i+1} N_{2i+1}.$$

One can also find the dominant eigenvalue as

$$\lambda_0 = \lim_{k \rightarrow \infty} \frac{1}{\Delta t} \log \left( \frac{\sum_{i=1}^I n_i^{k+1}}{\sum_{i=1}^I n_i^k} \right).$$

For matrices with one dominant eigenvalue and a corresponding one-dimensional eigenspace, it is known that the power algorithm is fast and in fact converges with exponential rate [26]. In practice, we can stop the iterations when the relative error on the normalized quantity

$$\frac{1}{\Delta t} \left( \sum_{i=1}^I \tilde{n}_i^{k+1} - \sum_{i=1}^I \tilde{n}_i^k \right)$$

is small enough, say of the order of  $10^{-10}$ .

### 3.2. Inverse problem: general strategy

In the following, we denote by  $H$  the product  $B \cdot N$  and its approximations. Indeed, from equations (6) or (11), we have to search for the product  $H = B_{\varepsilon,\alpha} N_\varepsilon$  or  $H = B_{\varepsilon,\alpha} N_{\varepsilon,\alpha}$  before computing  $B_{\varepsilon,\alpha}$ . In particular, we cannot avoid a loss of information where  $N_\varepsilon$  is small, i.e., for  $x \approx 0$  or  $x \gg 1$ .

The inverse problem (5), as well as (11), can be written as

$$4H(2x) - H(x) = L(x), \tag{22}$$

with different expressions for  $H$  and  $L$ . We may think of two possible numerical approaches.

**Strategy 1.** Compute  $H(2x)$  from  $H(x)$ : this means that we rewrite equation (22) with the new variable  $y = 2x$ , and arrive at

$$4H(y) - H\left(\frac{y}{2}\right) = L\left(\frac{y}{2}\right). \tag{23}$$

The scheme departs from zero, and one deduces the values of  $H_i$  step by step, from knowledge of  $H_j$  for  $j \leq i - 1$ .

**Strategy 2.** Compute  $H(x)$  from  $H(2x)$ : the scheme departs from the largest point  $x = L$  of our simulation domain. We suppose that for  $x \geq L$  we have  $H(x) = H(L) = 0$  (it is relevant since we suppose that  $N$  vanishes for  $x$  large: see below), and then deduce the smaller values  $H_i$  step by step, from knowledge of  $H_j$  for  $j \geq i + 1$ .

The two approaches do not necessarily lead to the same result because the continuous equation

$$4H(2x) - H(x) = 0 \tag{24}$$

has infinitely many solutions. This issue is interesting on its own and is related to the construction of wavelets, see [27]. It is discussed in proposition [appendix A.1](#).

By imposing  $H \in L^2(\mathbb{R}_+)$ , we select a unique solution, as shown in theorem [appendix A.3](#). The question is then: which numerical strategy should we use to select the *correct* solution, i.e. the one in  $L^2(\mathbb{R}_+)$ ?

Among the solutions of equation (22), we single out two, defined by the power series:

$$H^{(1)}(x) = \sum_{n=1}^{+\infty} 2^{-2n} L(2^{-n}x) \quad \text{and} \quad H^{(2)}(x) = - \sum_{n=0}^{+\infty} 2^{2n} L(2^n x), \quad \forall x > 0.$$

Proposition [appendix A.1](#) shows that for  $L \in L^2(\mathbb{R}_+, x^p dx)$ , there is a unique solution in  $L^2(\mathbb{R}_+, x^p dx)$ , given by  $H^{(1)}$  if  $p < 3$  and by  $H^{(2)}$  if  $p > 3$  (and the power series converge in the corresponding spaces).

For  $B > 0$  smooth and bounded from above and below, we know that  $N$  is smooth and vanishes at  $x \approx 0$  and  $x \approx \infty$ , and  $BN$  inherits these properties. For instance, we know that

$H \in L^2(dx) \cap L^2(x^4 dx)$ . By uniqueness of a solution in each space, proposition [appendix A.1](#) implies that  $H^{(2)} = H^{(1)}$ , or equivalently:

$$\sum_{n=-\infty}^{+\infty} 2^{2n} L(2^n x) = 0, \quad \forall x \geq 0.$$

This very particular property cannot be verified at the discrete level. Hence, the two strategies generally give two different approximations of the same solution of (22). The first strategy selects an approximation of the solution  $H^{(1)}$ , whereas the second selects an approximation of the solution  $H^{(2)}$ . In the case of a very regular data  $N$ , then  $H^{(2)}$  will perform better around infinity, whereas  $H^{(1)}$  will be better around zero. However, if  $N$  is a solution of equation (2), when we increase the number of points, the two approaches converge to the same solution since  $H^{(2)} = H^{(1)}$ .

Since our simulation domain  $[0, L]$  is bounded and contains zero, we prefer the first strategy. This choice is confirmed by all the numerical tests we have performed: the second approach has always lead to a solution exploding around zero. However, for the sake of completeness, we also describe the scheme we used for the second approach.

### 3.3. Inverse problem: filtering approach

According to strategies 1 and 2, we now present two approaches to handle the numerical solution of the inverse problem regularized with the *filtering approach*. Both need to first compute the convolution terms arising in (11). To do so we first take the fast Fourier transform  $F$  of  $N_\varepsilon$ , multiply it by  $i\xi \hat{\rho}_\alpha(\xi)$ , and then take the inverse fast Fourier transform  $F^*$ . We choose and define the regularization function  $\rho_\alpha$  by its Fourier transform:

$$\hat{\rho}_\alpha(\xi) = \frac{1}{\sqrt{1 + \alpha^2 \xi^2}}.$$

This leads us to the numerical approximation

$$\frac{\partial}{\partial x} N_{\varepsilon, \alpha} \approx dN_\alpha = F^*(i\xi \hat{\rho}_\alpha(\xi) F(N_\varepsilon)(\xi)). \quad (25)$$

We also impose  $dN_{\alpha, 0} = 0$  for compatibility with the continuous equation and further use.

As mentioned earlier, there are two alternatives, either starting from zero or coming from infinity.

**3.3.1. The Filtering approach starting from zero (strategy 1).** We solve equation (11) considered as an equation in the variable  $y = 2x$ , that is to say (23), in order to compute its solution  $H^{(1)}(x)$ . At the discrete level, we use the notations

$$H_i^f \approx B_i N_i, \quad L_i^f = dN_{\alpha, i} + \lambda_{\varepsilon, \alpha} N_i, \quad L_0^f = 0.$$

The discrete version of (23) reads

$$4H_i^f = H_{\frac{i}{2}}^f + L_{\frac{i}{2}}^f, \quad \forall 0 \leq i \leq I. \quad (26)$$

Furthermore, for an arbitrary sequence  $G_i, i = 1, 2, \dots, \infty$  we need to define the quantities  $G_{\frac{i}{2}}$ . We choose

$$G_{\frac{i}{2}} = \begin{cases} G_{\frac{i}{2}} & \text{when } i \text{ is even,} \\ \frac{1}{2}(G_{\frac{i-1}{2}} + G_{\frac{i+1}{2}}) & \text{when } i \text{ is odd.} \end{cases} \quad (27)$$

In particular, we have  $H_0^f = 0$ .

Adding up all the terms in (26) for  $1 \leq i \leq I$ , we find (with  $I$  even to simplify):

$$4 \sum_{i=0}^I H_i^f = 2 \sum_{i=0}^{\frac{I}{2}} (H_i^f + L_i^f) - \frac{1}{2} (H_{I/2}^f + L_{I/2}^f).$$

Since we have assumed that  $N$  has exponential decay for  $x \gg 1$ , it follows that

$$\sum_{i=0}^I H_i^f = \sum_{i=1}^I L_i^f + E_I \quad \text{with} \quad |E_I| \leq 2 \sum_{i=\frac{I}{2}}^I |H_i|. \tag{28}$$

Multiplying (26) by  $x_i$  and summing up again, we find

$$\sum_{i=1}^{\frac{I}{2}} x_i L_i^f = F_I \quad \text{with} \quad |F_I| \leq \sum_{i=\frac{I}{2}}^I x_i |H_i|. \tag{29}$$

As a consequence, we can choose

$$\lambda_{\varepsilon, \alpha} = - \frac{\sum x_i dN_{\alpha, i}}{\sum x_i N_i}, \tag{30}$$

as the discrete version of relations (4) or (12).

3.3.2. *The filtering approach starting from infinity (strategy 2).* Another method is to discretize the formulation (22) in order to compute its solution  $H^{(2)}(x)$ . We define the extension  $H_i^f = 0$  for  $i \geq I + 1$ , and for  $2 \leq i \leq I$ , we define by backward iterations

$$H_i^{f\infty} = 2H_{2i}^{f\infty} + H_{2i+1}^{f\infty} + H_{2i-1}^{f\infty} - L_i^f. \tag{31}$$

This however does not apply to the indices  $i = 0, 1$  and we set  $H_0^f = \frac{L_0^f}{3} = 0$  and  $H_1^f = 4H_2^f - L_1^f$ . By summing up all the terms in (31), we find balance properties equivalent to (28) and (29), but with remainders  $E_I$  and  $F_I$  depending on  $H_1$  and  $H_2$  instead of  $H_{i \geq \frac{I}{2}}$ . One has to check *a posteriori* that these last quantities are very small; it is not the case in a standard calculation, but becomes true when the precision of the direct problem scheme increases.

3.4. *Inverse problem: quasi-reversibility approach*

In this section, we present a numerical scheme for the regularized inverse problem proposed in [1]. This problem leads to solving (6) taken at  $y = 2x$ , that is

$$\begin{cases} \alpha \frac{\partial}{\partial y} (B_{\varepsilon, \alpha} N_\varepsilon) + 4B_{\varepsilon, \alpha}(y) N_\varepsilon(y) = B_{\varepsilon, \alpha} \left( \frac{y}{2} \right) N_\varepsilon \left( \frac{y}{2} \right) + \lambda_{\varepsilon, \alpha} N_\varepsilon \left( \frac{y}{2} \right) \\ \quad + 2 \frac{\partial}{\partial y} \left( N_\varepsilon \left( \frac{y}{2} \right) \right), \quad y > 0, \\ (B_{\varepsilon, \alpha} N_\varepsilon)(0) = 0, \end{cases}$$

where  $\alpha > 0$  is the regularizing parameter and  $\lambda_{\varepsilon, \alpha}$  is defined by (9). This gives, in a discretized version, after dropping the index  $\varepsilon$ ,

$$\lambda_{\varepsilon, \alpha} = \frac{\sum N_i}{\sum x_i N_i + \frac{\alpha}{4} \sum N_i}. \tag{32}$$

For the numerical discretization we set  $H_{-1}^Q = 0$  and also recall that  $N_0 = 0$  and assume that the data satisfy  $N_{I+1} = 0$ . We use a standard upwind scheme for the differential term:

$$\frac{\alpha}{\Delta x} (H_i^Q - H_{i-1}^Q) + 4H_i^Q = H_{\frac{i}{2}}^Q + L_{\frac{i}{2}}^Q, \tag{33}$$

where we have defined the fractional indices as in the filtering approach by (27), and here

$$L_i^Q = \lambda_\varepsilon N_i + \frac{N_{i+1} - N_i}{\Delta x}.$$

If we neglect the terms  $H_{i \geq \frac{1}{2}+1}^Q$ , we can easily verify a discrete version of the balance laws (7) and (9), equivalent to (28) and (29).

#### 4. Numerical tests

As input data, we take the values of the function  $N$  obtained by the numerical solution of the direct problem in section 3.1, we add a random noise uniformly distributed in  $[-\frac{\varepsilon}{2}, \frac{\varepsilon}{2}]$ , and we enforce nonnegativity of the data

$$N_\varepsilon = \max(N + \varepsilon r, 0).$$

We solve the direct problem on a regular grid of  $I + 1$  points, on an interval  $[0, 2L]$ . We need  $L$  large enough, such that it is possible to assume that  $N(x \geq L) \approx 0$  and we have checked it *a posteriori*. Indeed, we have seen that this property is essential when we use the inverse schemes on a domain  $[0, L]$  in order to verify the balance laws (7)–(9). In other words, we solve the direct problem on a domain twice larger than for the inverse problem. In the numerical tests we take  $L = 4$ , and we show the numerical solution  $N$  only on the interval  $[0, L]$  since it is uniformly small on  $[L, 2L]$ .

We solve the inverse problem by the different methods on a regular grid of  $I_1 + 1$  points on  $[0, L]$ , with  $\Delta x_1 = L/I_1$ . This grid is taken ten times finer than the grid used for the direct problem, i.e. we take  $I_1 = 10I$ . Since we have chosen  $L$  large enough so that  $N(x \geq L) \approx 0$ , we have always obtained that indeed  $H(x \geq L) \approx 0$ .

As before, we denote by  $H^Q$  and  $H^f$  the solution data  $H$  obtained respectively by the quasi-reversibility method of section 3.4 and by the first filtering approach (from zero) of section 3.3. We also define a solution  $H^{fQ}$  by mixing both methods, i.e. by solving the following equation:

$$\begin{cases} \frac{\alpha_Q}{2} \frac{\partial}{\partial x} (B_{\varepsilon, \alpha_Q, \alpha_f} N_\varepsilon)(2 \cdot) + 4B_{\varepsilon, \alpha_Q, \alpha_f}(x) N_\varepsilon(2 \cdot) - B_{\varepsilon, \alpha_Q, \alpha_f} N_\varepsilon \\ = \left( \frac{\partial}{\partial x} N_\varepsilon + \lambda_{\varepsilon, \alpha_Q, \alpha_f} N_\varepsilon \right) * \rho_{\alpha_f}, \\ B_{\varepsilon, \alpha_Q, \alpha_f}(x = 0) N_\varepsilon(x = 0) = 0, \end{cases} \quad (34)$$

where  $\lambda_{\varepsilon, \alpha_Q, \alpha_f}$  is defined by

$$\lambda_{\varepsilon, \alpha_Q, \alpha_f} = \frac{\int_0^\infty N_\varepsilon * \rho_{\alpha_f} dx}{\int_0^\infty x N_\varepsilon * \rho_{\alpha_f} dx + \frac{\alpha_Q}{4} \int_0^\infty N_\varepsilon * \rho_{\alpha_f} dx}. \quad (35)$$

The relative error is measured, as seen in theorem 2.1 and in theorem 5.1 of [1], by

$$\delta^Q = \frac{\|BN_\varepsilon - H^Q\|_{L^2}^2}{\|N_\varepsilon\|_{L^2}^2}, \quad \delta^f = \frac{\|BN_\varepsilon - H^f\|_{L^2}^2}{\|N_\varepsilon\|_{L^2}^2}, \quad \delta^{fQ} = \frac{\|BN_\varepsilon - H^{fQ}\|_{L^2}^2}{\|N_\varepsilon\|_{L^2}^2}.$$

We have divided by  $\|N_\varepsilon\|_{L^2}$  and not by  $\|N\|_{H^2}$  because in practice we only know the entry data with noise.

In equation (35), we have carried out a number of tests for several values of  $\varepsilon$ , in order to find the optimal ratio  $\alpha_Q/\alpha_f$  for which the error  $\delta^{fQ}$  is minimal. It appears that this optimal ratio varies in the range  $[1/2, 4]$ , and it depends not only on the value of the noise level  $\varepsilon$  but also on the chosen profile  $B$ . Such uncertainty is due to the fact that when  $\alpha_Q$  and  $\alpha_f$  are

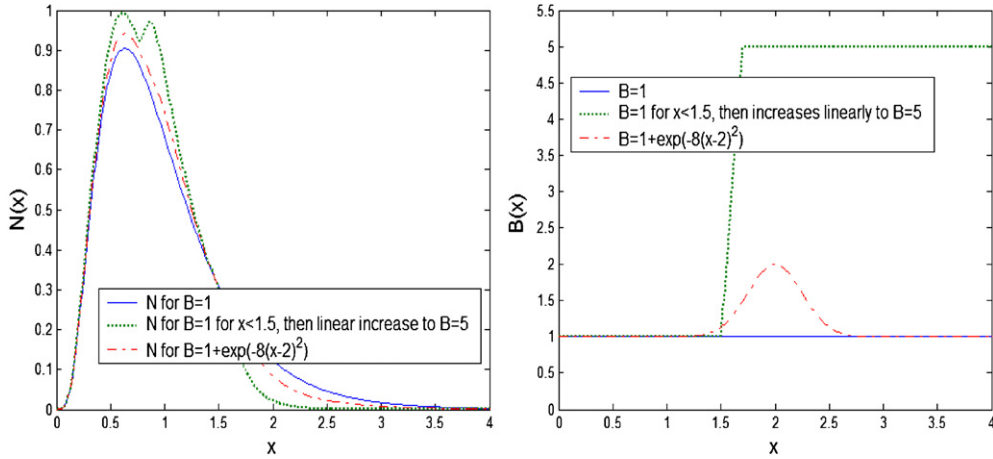


**Figure 1.** Solutions  $N$  (left) obtained by the numerical resolution of section 3.1 for the direct problem with three different division rates  $B$  (right).

in the optimal order of magnitude, the variation in the computed errors with the ratio is very small, and not really significant. Indeed, the error only varies a small percentage, making the imprecision due to the randomness of  $N_\varepsilon$  very prominent. For this reason, in the following, unless otherwise stated, we shall take  $\alpha_f = \alpha_Q = \alpha$ .

In order to illustrate the accuracy of our method, we also compare it to a naive way (brute force) of considering the equation. Namely, we approximate  $\frac{\partial}{\partial x} N(x)$  by a second-order Euler scheme without regularization. It gives a solution  $H^b$  by the same formula (33), where we simply take  $\alpha = 0$ .

#### 4.1. The direct problem

We have first tested the direct problem for various division rates  $B$ . Three different solutions  $N$  for three given division rates  $B$  are depicted in figure 1 with 800 grid points.

In the particular case when  $B$  is constant, we can go further and evaluate the computational error. Then, we know that  $\lambda = B$  and the exact solution  $N_{\text{exact}}$  can be explicitly calculated, as shown in [16, 3], by the formula:

$$N_{\text{exact}}(x) = \bar{N} \sum_{n=0}^{\infty} \alpha_n e^{-2^n Bx}, \quad (36)$$

where the coefficients are defined recursively by  $\alpha_0 = 1$  and  $\alpha_n = (-1)^n \frac{2\alpha_{n-1}}{2^n - 1}$ , and  $\bar{N}$  is chosen to ensure the mass one normalization. We take  $B = 1$  and obtain the continuous curve of figure 1. We can measure here the relative error by

$$\delta^D = \frac{\|N - N_{\text{exact}}\|_{L^1}}{\|N_{\text{exact}}\|_{L^1}},$$

where  $N$  represents the numerical solution of section 3.1. We choose this norm because for  $B$  constant, the solution of the adjoint problem is  $\phi = 1$  and the general relative entropy principle [3, 18] gives us that this quantity decreases along the time iterations. Still for 800 points, we obtain  $\delta^D = 7.7 \times 10^{-3}$ .

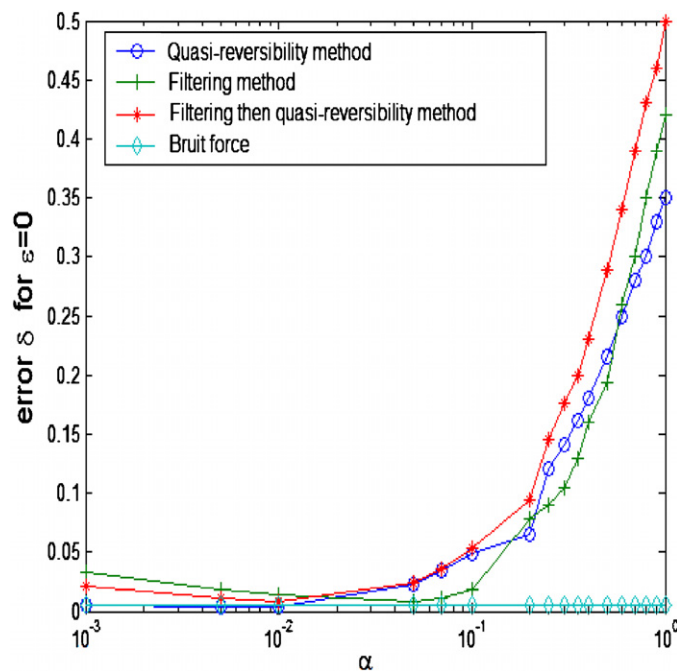


**Figure 2.** For  $\varepsilon = 0$ , numerical errors obtained with the different methods for the inverse problem. Note the  $L$ -shaped behavior of the computed error with respect to the regularization parameter.

#### 4.2. The noiseless case ( $\varepsilon = 0$ )

In the simplest case where the data are perfectly known, i.e. for  $\varepsilon = 0$ , we verify that the different schemes allow us to recover  $B$ . Since the precision of the data is directly linked to the number of points used in the scheme, we run the codes with 1.000 points for the direct problem (below, we will take only 100 points).

We test several values of  $\alpha$  and we use the three functions  $B$  of figure 1 for each method for the inverse problem. The error estimate is found to depend on the method used but not significantly on the division rate  $B$ . Therefore, we have drawn in figure 2 the average error estimates for the three division rates  $B$ . In figure 3 we have depicted the products  $B \cdot N$  in the case  $B = 1$  and  $\alpha = 0.01$  (other cases are similar): it shows that the precision obtained is satisfactory. In figures 4–6 we have drawn the approximations of  $B$  in each of the three cases, calculated only for  $N > 0.01$  (indeed, for  $N$  too small the division leads to insignificant results on  $B$ ).

Not surprisingly, the brute force method reveals to be satisfactory, with an error estimate of  $\delta^b = 1.3 \times 10^{-2}$ , since we are in the case where  $N$  is very regular. The filtering method can reach this level of error for  $\alpha = 10^{-2}$  but cannot go further. However, both the quasi-reversibility method and the mixed method given by equation (34) improve it with minimum values  $\delta^Q = 6.9 \times 10^{-3}$  and  $\delta^{fQ} = 6.5 \times 10^{-3}$  reached for  $\alpha = 10^{-2}$ .

#### 4.3. Link between the noise level $\varepsilon$ and the regularization parameter $\alpha$

For noise levels  $\varepsilon = 0.01$ ,  $\varepsilon = 0.05$  and  $\varepsilon = 0.1$  respectively, figures 7–9 give the curves  $\varepsilon$  as a function of  $\alpha$  for the three inverse methods. We compare the reconstructed division rates  $B$  in figures 10 and 11.

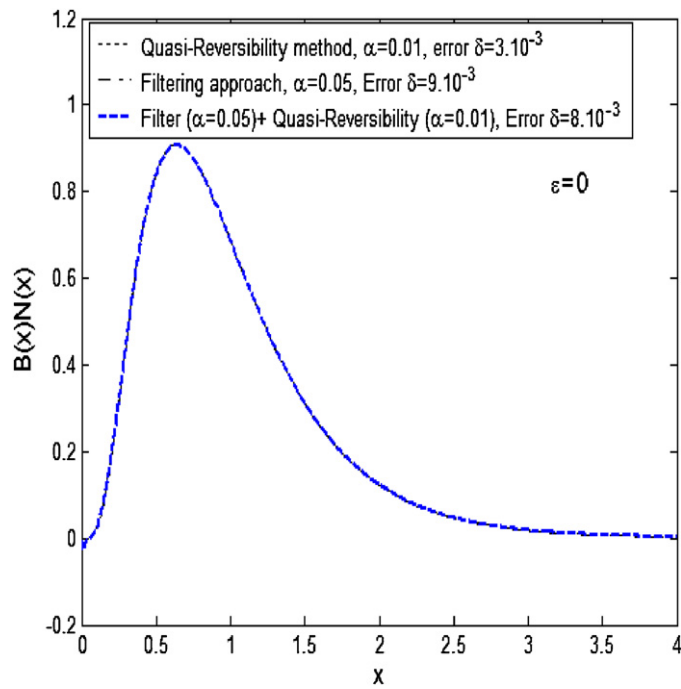


**Figure 3.** Numerical reconstruction of  $B \cdot N$  obtained by each method for the inverse problem when  $B = 1$ ,  $\varepsilon = 0$  and  $\alpha = 0.01$ .

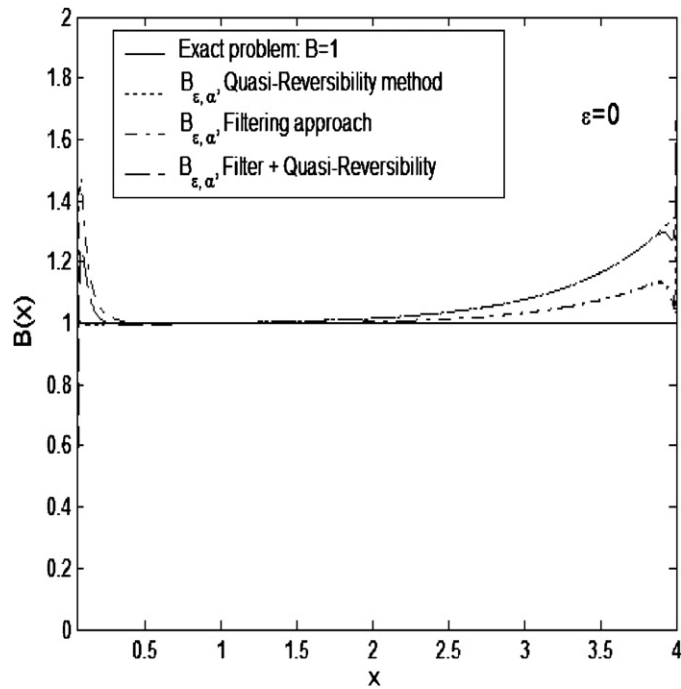


**Figure 4.** Reconstructed division rate  $B$  using the three inverse methods, for  $\varepsilon = 0$ ,  $\alpha = 0.01$  with  $N$  computed from  $B = 1$ .

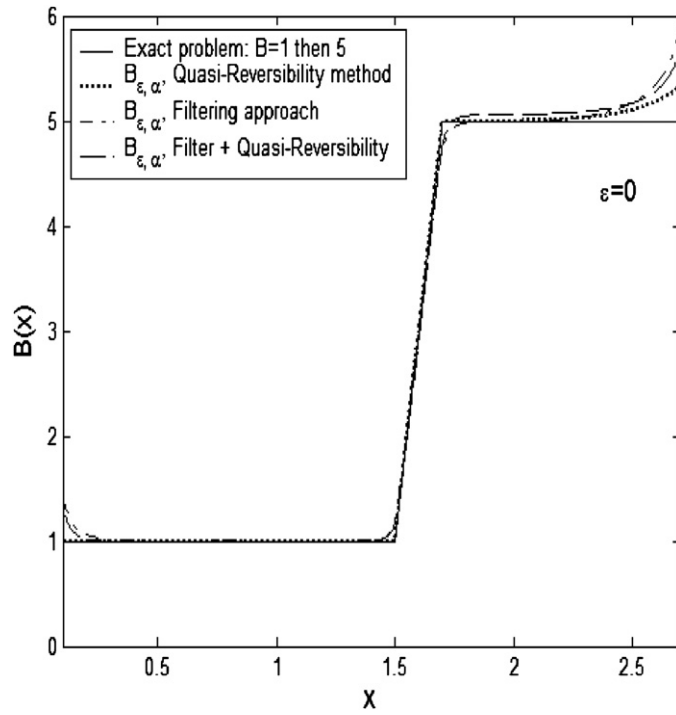


Figure 5. Reconstructed division rate  $B$ , for  $\varepsilon = 0$ ,  $\alpha = 0.01$  and a jump  $B = 1-5$  as in figure 1.

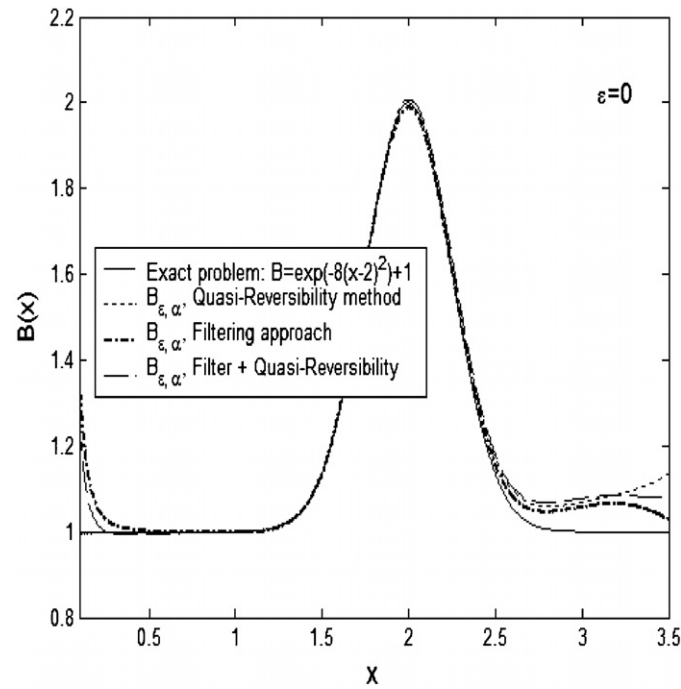


Figure 6. Reconstructed division rate  $B$ , for  $\varepsilon = 0$ ,  $\alpha = 0.01$  and  $B = 1 + \exp(-8(x - 2)^2)$ .

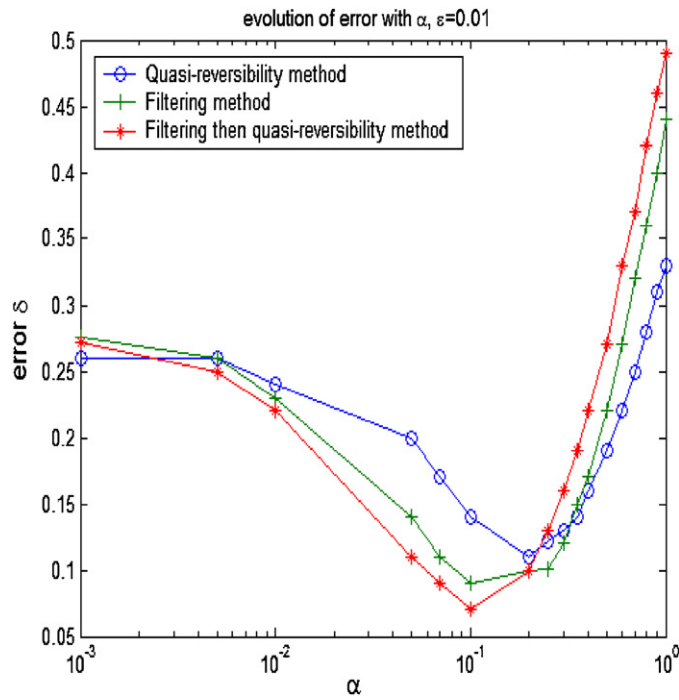


Figure 7. Numerical error when  $\epsilon = 0.01$  for the different methods.

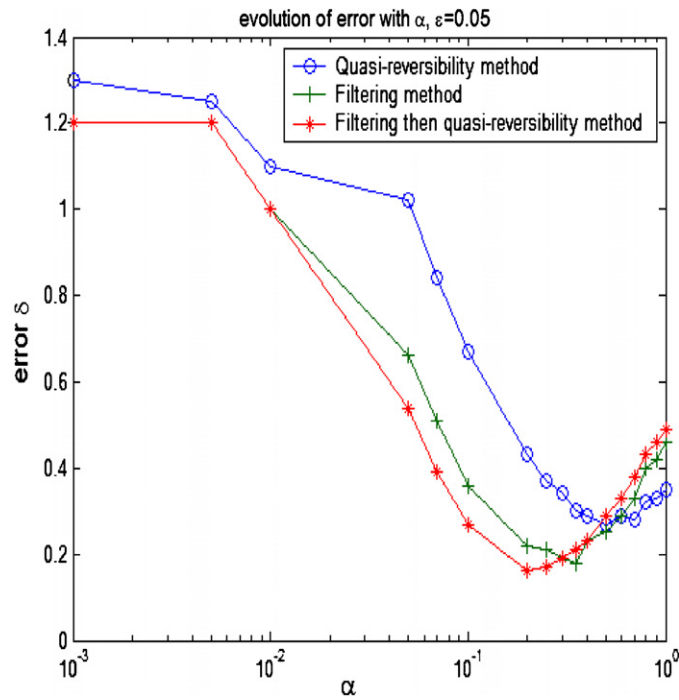


Figure 8. Numerical error when  $\epsilon = 0.05$ .

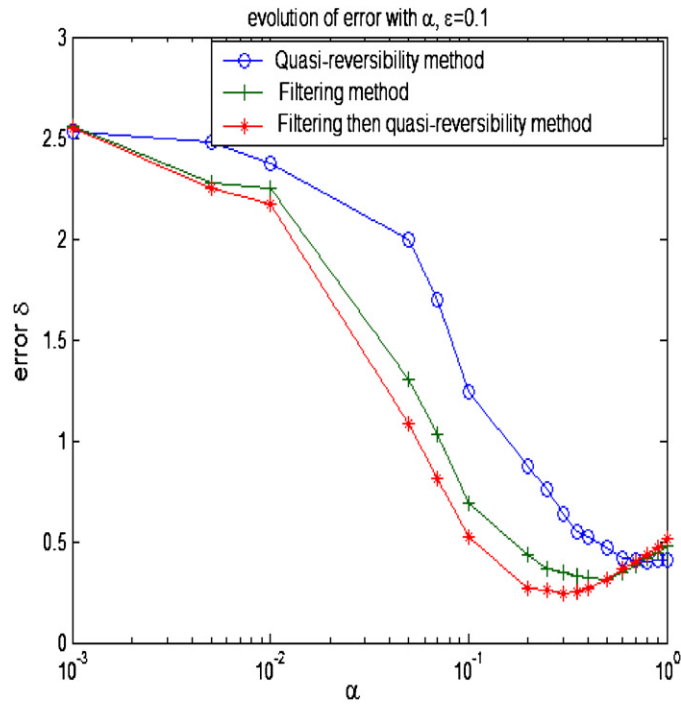


Figure 9. Numerical error when  $\varepsilon = 0.1$ .

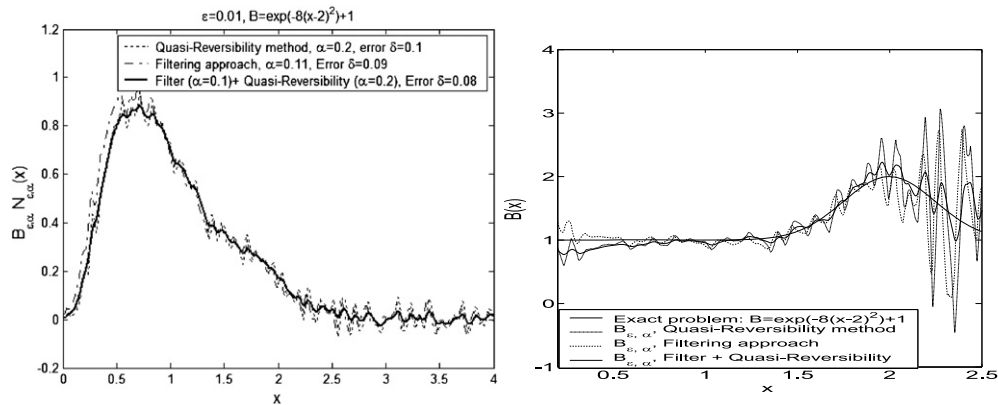


Figure 10. In the case  $\varepsilon = 0.01$ ,  $\alpha = 0.05$ ,  $B = 1 + e^{-8(x-2)^2}$ , numerical solution  $B \cdot N$  (left) and  $B$  (right) by the different methods.

Each of the error curves presents a minimum for an optimal value of  $\alpha$ , as expressed by estimate (13) for instance. In figures 12–15, we have compared three curves, drawn in a log–log scale:  $\sqrt{\varepsilon}$  to serve as a reference curve,  $f(\varepsilon) = \min_{\alpha} \delta(\alpha, \varepsilon)$ , and  $g(\varepsilon) = \arg \min_{\alpha} \delta(\alpha, \varepsilon)$ . One can see that for each method, these three curves have comparable slopes ( $\frac{1}{2}$  on a log–log scale): they show that even though the combination of filtering and quasi-reversibility method improves the optimal errors in absolute value, it does not change the order of convergence

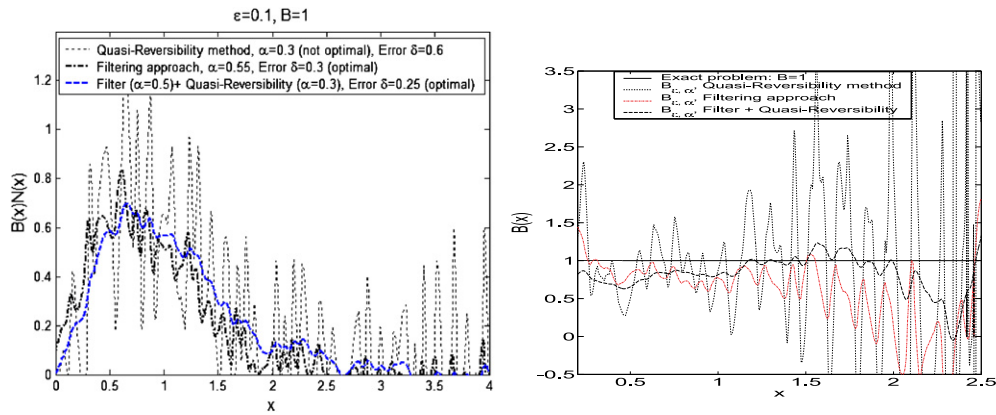


Figure 11. In the case  $\varepsilon = 0.1$  and  $B = 1$ , the numerical solution  $B \cdot N$  (left) and  $B$  (right) by the different methods.

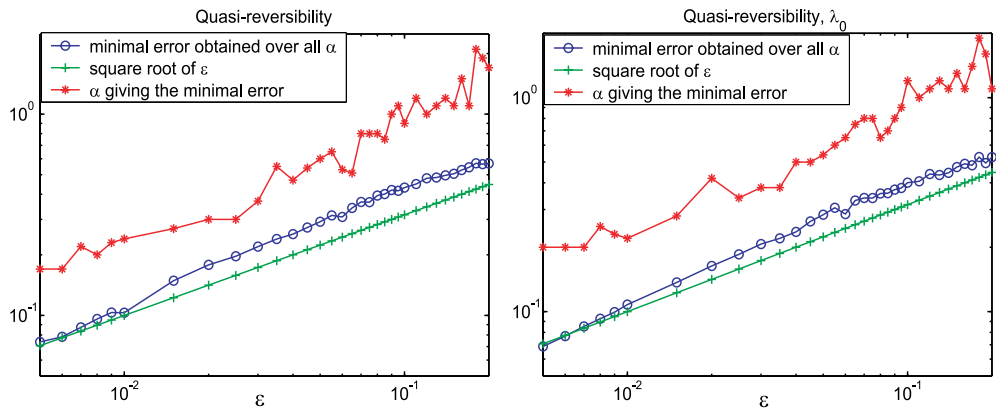


Figure 12. Quasi-reversibility method, with (left)  $\lambda_{\varepsilon,\alpha}$  given by relation (9) or (right) *a priori* knowledge of  $\lambda_0$ : minimal error and optimal regularization parameter  $\alpha$  as functions of the noise level  $\varepsilon$ , with a comparison to the theoretical curve  $\sqrt{\varepsilon}$ . We see that the *a priori* knowledge of  $\lambda_0$  does not improve the speed of convergence of the scheme.

of the approximation, which remains of order  $O(\sqrt{\varepsilon})$ . Figure 14 gives also the convergence of the filtering method for much smaller values of  $\varepsilon$  (for which an increased number of 500 points has been taken, in order to avoid numerical bias): the comparison with  $\sqrt{\varepsilon}$  is there particularly evident, and we have obtained similar curves for the two other methods. The speed of convergence is therefore in complete accordance with the theoretical estimate in equation (13). Moreover, our three methods still work for very high levels of noise, even up to 100%. This is illustrated, for the quasi-reversibility method, in figure 16.

4.4. Influence of the choice of  $\lambda_0$  instead of  $\lambda_{\varepsilon,\alpha}$

To evaluate the influence of the error term due to the distance  $|\lambda_{\varepsilon,\alpha} - \lambda_0|$ , we compare the curves obtained respectively by taking the inverse code of the exact  $\lambda_0$  or the value  $\lambda_{\varepsilon,\alpha}$  expressed by the balance laws. They are drawn in figure 12 for the quasi-reversibility method.

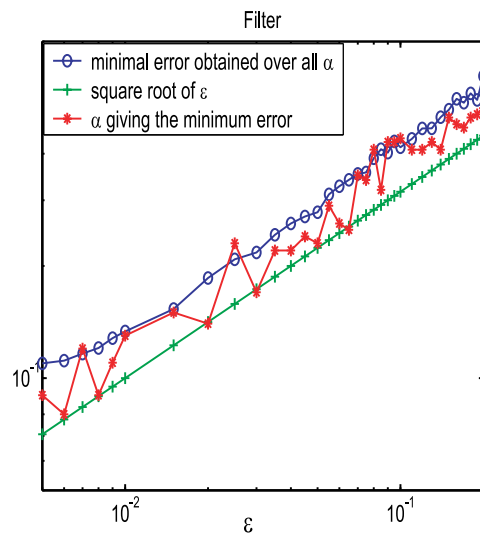


Figure 13. Filtering method for standard levels of noise.

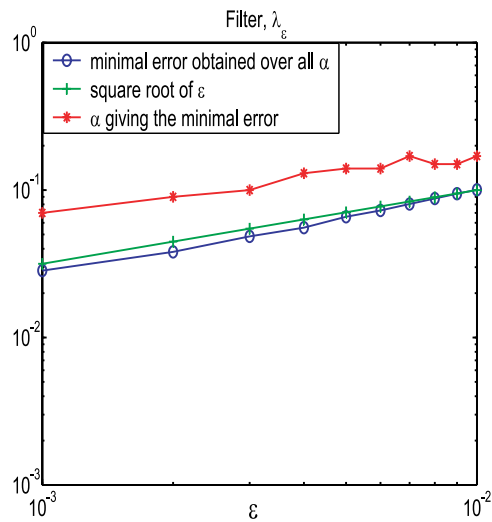
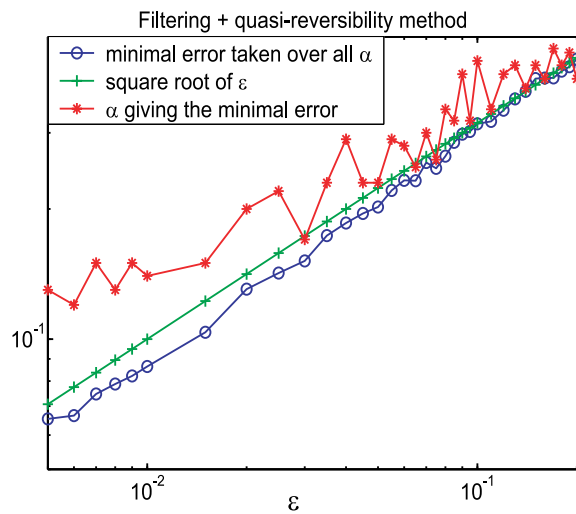


Figure 14. Filtering method for smaller values of  $\varepsilon$  and increased number of points.

They show that even though the *a priori* knowledge of  $\lambda_0$  improves the error in absolute value, it does not change the order of convergence of the scheme. Thus it is in complete accordance with estimate (13).

#### 4.5. Comparison between the three methods and discussion on oscillations

As already discussed, the combination of filtering and quasi-reversibility method improves the optimal errors in absolute value, even if it does not change the order of convergence of the approximation. Another advantage of this combined method lies in the fact that it diminishes



**Figure 15.** Filtering and quasi-reversibility combined method: minimal error as a function of the noise level  $\varepsilon$  for the optimal value  $\alpha$ , with a comparison to the theoretical curve  $\sqrt{\varepsilon}$ .

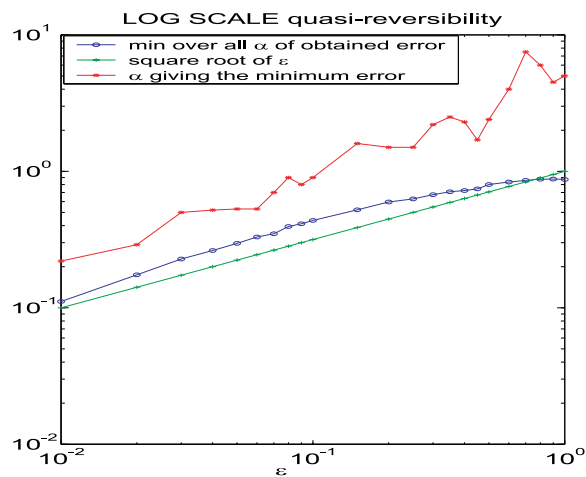


**Figure 16.** Quasi-reversibility method for high values of the noise level: the method continues to work very well even for very high noise.

oscillations. Indeed, figures 10 and 11 show that some spurious oscillations occur for large  $x$  (i.e. for  $x > 2$ ), but that they are significantly reduced by the combined method.

First, oscillations are the consequence of our choice to simulate the noise by adding a random variable at each spatial step. It is indeed clear in the simulations that the smaller the spatial step size, the smaller the period of chaotic oscillations.

Second, since  $N$  being very small for  $x$  large, the recovered  $B$  becomes meaningless: we divide by a too small quantity, what emphasizes oscillations.

Finally, the fact that oscillations are more amplified for  $x$  large seems to be linked with our choice of a scheme that departs from zero and not from infinity (cf the results of

the appendix). Indeed, none of these two choices (departing from zero or from infinity) can be fully satisfactory, since lemma A.2. gives a kind of non-uniqueness result for any approximation.

By choosing to depart from zero, we privileged the results around zero, and accept the fact that our method could fail for large  $x$ . We based our choice on the mathematical analysis of appendix A, as explained in section 3.2. From a biological point of view also this choice seemed more relevant, since by simulating the direct problem, it appears clearly that even big changes in the value of  $B(x)$  appearing for large values of  $x$  do not change much the distribution  $N$ —in contrast to changes of  $B$  for small values of  $x$ .

A possible direction of future research could be to mix both schemes, the one from infinity and the other from zero, or to apply successively one and then the other, in order to remove or diminish spurious oscillations.

## 5. Conclusions

We have considered size-structured equations connected to several areas of biology from cell division to prion proliferation by aggregation and fragmentation. We have addressed the numerical efficiency of some inverse problem solution methods to tackle the problem of recovering the division rate from the size distribution of cells. The latter involves a dilation equation with a singular right-hand side that needs regularization for actual implementation. For that purpose, we have introduced a filtering method and proved its convergence for noisy data. This method brings in an operator that has a non-trivial kernel and we have chosen a numerical approximation that is able to select the biologically relevant solutions.

The implementation of the inverse algorithm, based on the filtering method, confirms the convergence analysis. In particular, there is an optimal regularization parameter as can be seen in the graphs of figures 7, 8 or 9 for instance. Comparison with a quasi-reversibility method introduced earlier leads to the conclusion that a combination of filtering and quasi-reversibility methods seems to be more efficient because the oscillations are reduced, but without improving the rate of convergence.

We also analyzed the impact of using the exact value of  $\lambda_0$  or the  $\lambda_\varepsilon$  on the different solutions of the inverse problem. In our simulations, the difference between using  $\lambda_0$  or  $\lambda_\varepsilon$  seemed to be immaterial as far as the accuracy of method is concerned. This is in perfect accordance with the theoretical estimate (13).

The above remarks open several directions for continuation and extension of the present work. On the practical side, the present work sets the stage for the use of experimental data either from the existing literature or from more recent biological experiments. On the theoretical side, the possibility of improving the convergence by combining the filtering and quasi-reversibility methods should be investigated further.

Finally, yet another natural continuation of the present work would be to analyze the computational complexity of the methods presented here *vis a vis* more standard techniques such as minimization coupled with Tikhonov regularization.

## Acknowledgments

The authors were supported by the CNPq-INRIA agreement INVEBIO. JPZ was supported by CNPq under grants 302161/2003-1 and 474085/2003-1. JPZ and BP are thankful to the RICAM special semester and to the International Cooperation Agreement Brazil–France. Part of this work was conducted during the Special Semester on Quantitative Biology Analyzed

by Mathematical Methods, 1 October 2007–27 January 2008, organized by RICAM, Austrian Academy of Sciences.

### Appendix A. Well-posedness of the functional equation associated with the inverse problem

We have seen that the regularization method for the inverse problem relies mostly on solving the equation

$$4H(2x) - H(x) = L(x), \quad x \geq 0. \quad (\text{A.1})$$

Even though this equation is formally very simple, its analysis reveals some complexity. It may admit several solutions in general. Among them, we can mention two with simple representation formulae (we leave to the reader to check they are indeed formally solutions)

$$H^{(1)}(x) = \sum_{n=1}^{+\infty} 2^{-2n} L(2^{-n}x), \quad (\text{A.2})$$

$$H^{(2)}(x) = - \sum_{n=0}^{+\infty} 2^{2n} L(2^n x). \quad (\text{A.3})$$

To clarify this issue and motivate our choice of a solution, we first state general results concerning solutions to (A.1) and then come back to our original problem (5).

We first mention the following.

**Proposition appendix A.1.** *Let  $L \in L^2(\mathbb{R}_+, x^p dx)$ , with  $p \neq 3$ , then there exists a unique solution  $H \in L^2(\mathbb{R}_+, x^p dx)$  to (A.1) and*

- for  $p < 3$ , this solution is given explicitly by formula (A.2). Furthermore, for  $1 \leq q \leq \infty$ , if  $L \in L^q(\mathbb{R}_+)$  then  $H^{(1)} \in L^q(\mathbb{R}_+)$ ;
- for  $p > 3$ , this solution is given explicitly by formula (A.3).

Because we look for an integrable function  $H$  (the number of cells is supposedly finite), the function  $H^{(1)}$  is preferable (take  $q = 1$ ). It also behaves better near  $x \approx 0$  because the weight  $p < 3$  imposes that  $H^{(1)}$  vanishes at 0 as we expect.

From the point of view of exact solutions of the direct problem, we find that  $H = BN$  and  $L$  belong to all spaces  $L^2(\mathbb{R}_+, x^p dx)$  for all  $p \in \mathbb{R}$ . Therefore, the two solutions coincide and in principle we could choose any of them. In practice, errors on the data  $L$  are better handled by  $H^{(1)}$  than by  $H^{(2)}$  for the afore-mentioned reason. Note indeed that these two solutions are different in general. One can check for instance that for  $L = 0$ , there is a singular distributional solution  $\delta'_{x=0}$ . Furthermore,

**Lemma appendix A.2.** *The solutions to (A.1) with  $L = 0$  in  $\mathcal{D}'(0, \infty)$  have the form  $\frac{f(\log(x))}{x^2}$  with  $f \in \mathcal{D}'(\mathbb{R})$  a  $\log(2)$ -periodic distribution.*

**Proof of proposition appendix A.1.** We consider the Hilbert space  $X = L^2(\mathbb{R}_+, x^p dx)$  and we simply apply the Lax–Milgram theorem to a properly chosen bilinear form.

**Case 1,  $p < 3$ .** We solve the equation in the variable  $y = 2x$  that is (23) and consider the bilinear form  $a(u, v)$  on  $X \times X$  defined by

$$a(u, v) = 4 \int_0^\infty u(y)v(y)y^p dy - \int_0^\infty u\left(\frac{y}{2}\right)v(y)y^p dy.$$

This form is obviously continuous and it remains to prove that it is coercive. We have

$$a(u, u) = 4 \int_0^\infty u(y)^2 y^p dy - \int_0^\infty u\left(\frac{y}{2}\right) u(y) y^p dy \geq (4 - 2^{\frac{p+1}{2}}) \int_0^\infty u(y)^2 y^p dy,$$

and it is indeed coercive as long as  $\alpha = 4 - 2^{\frac{p+1}{2}}$  is positive which holds true for  $p < 3$ . The Lax–Milgram theorem asserts that there is a unique  $H \in X$  such that  $a(H, \cdot) = (L, \cdot)$ , where  $(\cdot, \cdot)$  denotes the inner product in  $X$ , that is a solution of (23).

**Case 2,  $p > 3$ .** We work in the variable  $x$  and consider the continuous bilinear form  $b(u, v)$  on  $X \times X$  defined by

$$b(u, v) = -4 \int_0^\infty u(2x)v(x)x^p dx + \int_0^\infty u(x)v(x)x^p dx.$$

The same calculation leads us to

$$b(u, u) \geq \alpha \int_0^\infty u(x)^2 x^p dx, \quad \text{with } \alpha = 1 - 2^{\frac{3-p}{2}} > 0,$$

and the same conclusion holds.

To check formulae (A.2) and (A.3), it remains to prove that these solutions belong to the corresponding spaces:

$$\|H^{(1)}\|_{L^2(\mathbb{R}_+, x^p dx)} \leq \sum_{n=1}^\infty 2^{-2n} \|L(2^{-n}x)\|_{L^2(\mathbb{R}_+, x^p dx)} = \sum_{n=1}^\infty 2^{\frac{n}{2}(p-3)} \|L(x)\|_{L^2(\mathbb{R}_+, x^p dx)}.$$

This sum converges iff  $p > 3$ . In the same way, we write

$$\|H^{(2)}\|_{L^2(x^p dx)} \leq \sum_{n=0}^\infty 2^{2n} \|L(2^n x)\|_{L^2(\mathbb{R}_+, x^p dx)} = \sum_{n=0}^\infty 2^{\frac{n}{2}(3-p)} \|L(x)\|_{L^2(\mathbb{R}_+, x^p dx)},$$

which converges iff  $p > 3$ . □

**Proof of lemma appendix A.2.** When  $L = 0$ , we first define  $\mathcal{H} \in \mathcal{D}'(0, \infty)$  as the second antiderivative of  $H$ , and note that it should verify

$$\mathcal{H}(2x) = \mathcal{H}(x).$$

We perform the change of variables  $y = \log(x)$  and note that, if  $\mathcal{H} \in \mathcal{D}'(0, \infty)$ , it is equivalent to look for solutions  $f \in \mathcal{D}'(\mathbb{R})$  of

$$f(y + \log(2)) = f(y). \tag{A.4}$$

Hence, all the solutions in  $\mathcal{D}'(0, \infty)$  are given by  $\frac{f(\log(x))}{x^2}$ , where  $f \in \mathcal{D}'(\mathbb{R})$ . □

To conclude this appendix, we come back to our original problem (5) and draw the consequences in terms of  $B$ , not  $H$ .

**Theorem appendix A.3.** Let  $N \in L^2(\mathbb{R}_+)$ , with  $N(x) > 0$  for  $x > 0$ . Let  $L \in L^2(\mathbb{R}_+)$ . There exists a unique  $B \in L^2(\mathbb{R}_+, N^2 dx)$  solution of

$$4B(2x)N(2x) - B(x)N(x) = L(x). \tag{A.5}$$

**Proof.** The theorem follows directly from proposition appendix A.1 for  $p = 0$ , and since  $N > 0$ , we can define  $B = H/N$  for  $B \in L^2(\mathbb{R}_+, N^2 dx)$ . □

This theorem shows that we can find a solution  $B$  of (5) for all  $N$  and all  $\lambda$ , this is the basis of our algorithm. However, if we want that the solution  $B$  belongs to the space  $L^1(\mathbb{R}_+; xN(x) dx)$ , integration of (A.5) multiplied by  $x$  shows that  $L$  has to satisfy the condition

$$\int_0^\infty xL(x) dx = 0.$$

Applying this to equation (5), we recover that  $\lambda_0 = \int_0^\infty N(x) dx / \int_0^\infty xN(x) dx$ . In the case of equations (6) and (11) respectively, we get formulae (9) and (12), which discrete versions are expressed by (32) and (30).

In view of these considerations, it is better to use a discrete scheme defined by a matrix  $A$  that preserves a similar discrete property. Namely, for all  $H = (H_i)$ , we should have  $\sum_i i(AH)_i = 0$ , in other words the vector of components  $i$  belongs to the kernel of the adjoint of  $A$ . Indeed, this property yields the (discrete) regularity  $H \in L^1(\mathbb{R}_+; x dx)$ .

## References

- [1] Perthame B and Zubelli J P 2007 On the inverse problem for a size-structured population model *Inverse Problems* **23** 1037–52
- [2] Metz J A J and Diekmann O 1986 Formulating models for structured populations *The Dynamics of Physiologically Structured Populations (Amsterdam, 1983) (Lecture Notes Biomath. vol 68)* (Berlin: Springer) pp 78–135
- [3] Perthame B 2007 Transport equations arising in biology *Frontiers in Mathematics* (Basle: Birkhauser)
- [4] Engl H W, Rundell W and Scherzer O 1994 A regularization scheme for an inverse problem in age-structured populations *J. Math. Anal. Appl.* **182** 658–79
- [5] Gyllenberg M, Osipov A and Päivärinta L 2002 The inverse problem of linear age-structured population dynamics *J. Evol. Eqns* **2** 223–39
- [6] Rundell W 1989 Determining the birth function for an age structured population *Math. Popul. Stud.* **1** 377–395, 397
- [7] Pilant M and Rundell W 1991 Determining a coefficient in a first-order hyperbolic equation *SIAM J. Appl. Math.* **51** 494–506
- [8] Carrillo J A and Goudon T 2004 A numerical study on large-time asymptotics of the Lifshitz–Slyozov system *J. Sci. Comput.* **20** 69–113
- [9] Collet J-F, Goudon T, Poupaud F and Vasseur A 2002 The Beker–Döring system and its Lifshitz–Slyozov limit *SIAM J. Appl. Math.* **62** 1488–500
- [10] Collet J-F, Goudon T and Vasseur A 1999 Some remarks on large-time asymptotic of the Lifshitz–Slyozov equations *J. Stat. Phys.* **77** 139–52
- [11] Laurençot P 2005 Convergence to self-similar solutions for a coagulation equation *Z. Angew. Math. Phys.* **56** 398–411
- [12] Laurençot P and Mischler S 2005 Liapunov functionals for Smoluchowski’s coagulation equation and convergence to self-similarity *Monatsh. Math.* **146** 127–42
- [13] Calvez V, Lenuzza N, Oelz D, Deslys J-P, Mouthon F, Laurent P and Perthame B 2008 Bimodality, prion aggregates infectivity and prediction of strain phenomenon arXiv:0802.2024
- [14] Masel J, Jansen V A A and Nowak M A 1999 Quantifying the kinetic parameters of prion replication *Biophys. Chem.* **77** 139–52
- [15] Greer M L, Pujo-Menjouet L and Webb G F 2006 A mathematical analysis of the dynamics of prion proliferation *J. Theor. Biol.* **242** 598–606
- [16] Perthame B and Ryzhik L 2005 Exponential decay for the fragmentation or cell-division equation *J. Diff. Eqns* **210** 155–77
- [17] Michel P 2006 Existence of a solution to the cell division eigenproblem *Model. Math. Methods Appl. Sci.* **16** 1125–53
- [18] Michel P, Mischler S and Perthame B 2005 General relative entropy inequality: an illustration on growth models *J. Math. Pures Appl. (9)* **84** 1235–60
- [19] Baumeister J and Leitão A 2005 Topics in inverse problems 25<sup>o</sup> Colóquio Brasileiro de Matemática (25th Brazilian Mathematics Colloquium) of Instituto Nacional de Matemática Pura e Aplicada (IMPA), Rio de Janeiro (Rio de Janeiro: IMPA Mathematical Publications)

- [20] Engl H W, Hanke M and Neubauer A 1996 *Regularization of Inverse Problems (Mathematics and its Applications vol 375)* (Dordrecht: Kluwer)
- [21] Lattès R 1966 Non-well-set problems and the method of quasi reversibility *Functional Analysis and Optimization* (New York: Academic) pp 99–113
- [22] Lattès R and Lions J-L 1967 *Méthode de quasi-réversibilité et applications* Travaux et Recherches Mathématiques, Dunod, Paris
- [23] Bouchut F 2004 Nonlinear stability of finite volume methods for hyperbolic conservation laws, and well-balanced schemes for sources *Frontiers in Mathematics* (Basle: Birkhäuser)
- [24] LeVeque R J 2002 Finite volume methods for hyperbolic problems *Frontiers in Mathematics* (Cambridge: Cambridge University Press)
- [25] Godlewski E and Raviart P-A 1996 *Numerical Approximation of Hyperbolic Systems of Conservation Laws (Applied Mathematical Sciences vol 118)* (Berlin: Springer)
- [26] Serre D 2002 *Matrices: Theory and Applications (Graduate Texts in Mathematics vol 216)* (New York: Springer)
- [27] Strang G 1989 Wavelets and dilation equations: a brief introduction *SIAM Rev.* **31** 614–27